

# Chimera at the phase-flip transition of an ensemble of identical nonlinear oscillators

R. Gopal<sup>a</sup>, V. K. Chandrasekar<sup>a,\*</sup>, D. V. Senthilkumar<sup>c,\*\*</sup>, A. Venkatesan<sup>d</sup>, M. Lakshmanan<sup>b</sup>

<sup>a</sup>*Centre for Nonlinear Science & Engineering, School of Electrical & Electronics Engineering, SASTRA University, Thanjavur- 613 401, India.*

<sup>b</sup>*Centre for Nonlinear Dynamics, School of Physics, Bharathidasan University, Tiruchirapalli-620024, India*

<sup>c</sup>*School of Physics, Indian Institute of Science Education and Research, Thiruvananthapuram -695016, India*

<sup>d</sup>*Department of Physics, Nehru Memorial College, Puthanampatti, Tiruchirapalli 621 007, India*

---

## Abstract

A complex collective emerging behavior characterized by coexisting coherent and incoherent domains is termed as a chimera state. We bring out the existence of a new type of chimera in a nonlocally coupled ensemble of identical oscillators driven by a common dynamic environment. The latter facilitates the onset of phase-flip bifurcation/transitions among the coupled oscillators of the ensemble, while the nonlocal coupling induces a partial asynchronization among the out-of-phase synchronized oscillators at this onset. This leads to the manifestation of coexisting out-of-phase synchronized coherent domains interspersed by asynchronous incoherent domains elucidating the existence of a different type of chimera state. In addition to this, a rich variety of other collective behaviors such as clusters with phase-flip transition, conventional chimera, solitary state and complete synchronized state which have been reported using different coupling architectures are found to be induced by the employed couplings for appropriate coupling strengths. The robustness of the resulting dynamics is demonstrated in ensembles of two paradigmatic models, namely Rössler oscillators and Stuart-Landau oscillators.

*Keywords:* nonlinear dynamics, coupled oscillators, collective behavior

---

## 1. Introduction

An ensemble of coupled oscillators is a veritable black box exhibiting a plethora of complex cooperative dynamical behaviors mimicking several real world phenomena [1, 2, 3, 4]. Chimera state is such an intriguing emerging behavior that has been identified in an ensemble of identical oscillators with non-local coupling [5, 6, 7, 8, 9, 10, 11, 12, 13, 14, 15]. Since its identification, the notion of chimera has provoked a flurry of intense investigations because of the surprising fact that such an ensemble splits into two dynamically distinct domains, wherein all the oscillators evolve in synchrony in the coherent domain, while the oscillators in the incoherent domain evolve in asynchrony [16, 17, 18]. Earlier investigations on the phenomenon of chimera were restricted to nonlocal coupling, both in the weak and the strong coupling limits, giving rise to frequency [19, 20] and amplitude chimeras [21, 22, 20, 23, 24, 27, 28], as it was believed that nonlocal coupling is a prerequisite for the onset of chimera in an ensemble of identical oscillators. Later investigations revealed the emergence of chimera states under global coupling [29, 30, 31, 32], mean-field coupling [44] and even in nearest neighbor coupling [45, 46]. In addition to the frequency and amplitude chimeras, other types of chimera states such as amplitude mediated chimeras [47], intensity induced chimeras [48], and chimera death [22, 32, 40, 49, 50] were also reported in the recent literature. Further, the robustness of chimera states

---

\*Corresponding author

\*\*Corresponding author

*Email addresses:* chandru25nld@gmail.com (V. K. Chandrasekar), skumar@iisertvm.ac.in (D. V. Senthilkumar)

was reported in [23, 33], while chimera states and multi-cluster chimera states were also found in oscillators with time delayed feedback [34, 35, 36]. Very recently, different types of chimera states including imperfect chimera states and solitary states were also reported at the transition from incoherence to coherence [37, 39].

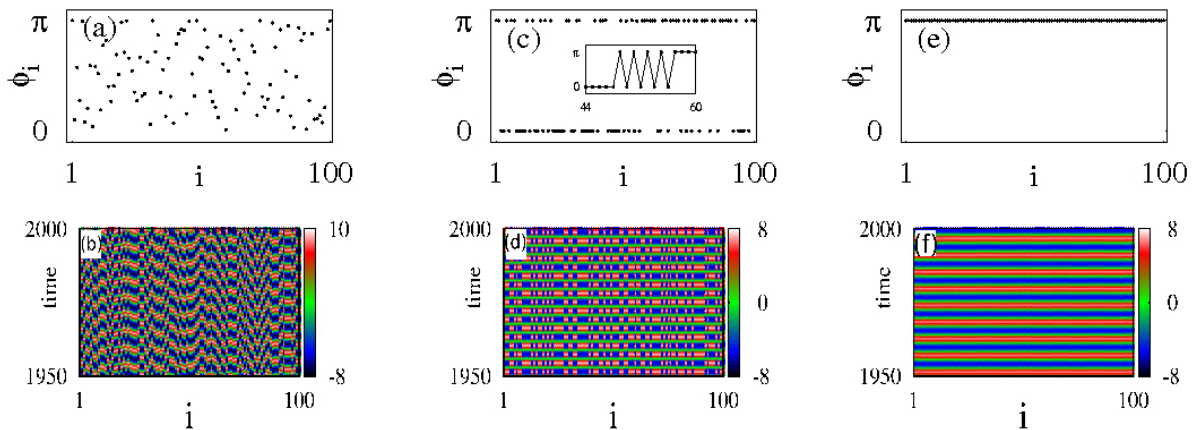


Figure 1: (Color online) Snapshots of instantaneous phases  $\phi_i = \arctan(y_i/x_i)$  (left column) and space-time plots of  $x_i$  (right column) of the Rössler oscillators (1) under the influence of the dynamic environment alone, with no nonlocal interaction (that is  $\epsilon = 0$ ). The parameters are fixed at  $a = 0.165$ ,  $b = 0.4$ ,  $c = 8.5$ ,  $k = 25$  and  $\eta = 2$  for different values  $q$  (a)-(b)  $q = 0.02$ , (c)-(d)  $q = 0.4$ , and (e)-(f)  $q = 1$ . The inset in Fig. 1(c) represents a two cluster state with phase-flip transition which is a special case of spatial chaos.

Notably, chimera states have also been demonstrated in laboratory experiments. In particular, chimera states have been discovered in populations of coupled chemical oscillators, in electro-optical systems [51, 52], electronic circuits [53] and in mechanical systems with two sub-populations of identical metronomes [54]. Surprisingly spatiotemporal patterns mimicking chimera states were also found in real world systems, which include the unihemispheric sleep of animals [55], the multiple time scales of sleep dynamics [56], and so on. Very recently, chimera states have also been reported in a network of two populations of Kuramoto model with inertia [57, 58], which is also a model used in the analysis of power grids [59]. Further investigations on identifying the intricacies involved in the mechanism of the onset of chimera states is of vital importance from the perspective of neuroscience because of the concept of “bumps” of neuronal activity [60, 62] associated with it.

In this paper, we report an interesting type of chimera arising out of the phase-flip bifurcation [68, 69, 70, 71] of an ensemble of identical oscillators. The coherent domains of the chimera state are out-of-phase synchronized with each other, whereas the incoherent domain is constituted by the asynchronous oscillators. Both the out-of-phase synchronized coherent domains and the incoherent domain coexist simultaneously in an ensemble of identical oscillators for suitable parameter values attributing to the existence of a new type of interesting chimera state, namely chimera at the phase-flip bifurcation/transition of the ensemble of oscillators. In addition to the above, clusters with phase-flip transition (*PFC*), conventional chimera, solitary state and complete synchronized states are also found to exist from the completely incoherent oscillator ensemble as a function of the coupling strength. We find that the phase-flip transition among the oscillators in the ensemble is induced by a common environmental coupling [64], while the chimera state in the ensemble is induced by the nonlocal coupling among the identical oscillators. The phenomenon of phase-flip bifurcation/transition was shown to be induced by a common environmental coupling in two coupled oscillators in the recent past [64]. Abrupt transition from in-phase to anti phase synchronized oscillations among the oscillators as a function of a system parameter, where their relative phase difference changes from zero to  $\pi$  at the bifurcation/transition point, is known as phase-flip bifurcation/transition [68, 69, 70]. The indirect coupling arising from the common medium or from the environment of the dynamical systems was shown to be a source of several collective behaviors of real world systems (see Ref. [63, 64, 65] and references

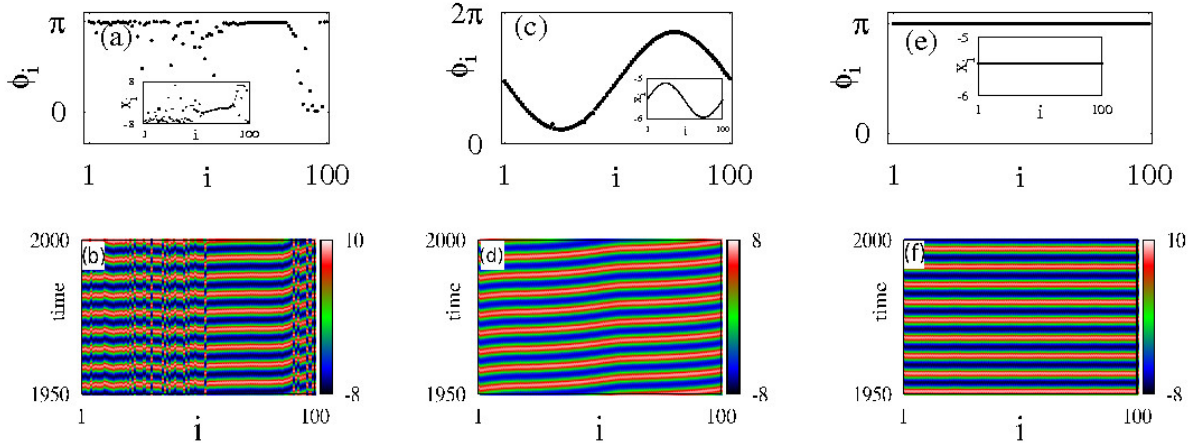


Figure 2: (Color online) Snapshots of the instantaneous phases  $\phi_i$  (left column) (of  $x_i$  are shown in the inset) and the space-time evolution of  $x_i$  (right column) of the ensemble of Rössler oscillators with  $q = 0.02$  for the coupling radius  $r = 0.3$  of the nonlocal coupling and for different values of the strength of the nonlocal coupling (a)-(b)  $\varepsilon = 0.01$ , (c)-(d)  $\varepsilon = 0.02$  and (e)-(f)  $\varepsilon = 0.05$ . Note that the insets in (b) and (c) correspond to the values of the variables  $x_i$ . The values of the other parameter are the same as in Fig. 1(a). Note that the insets depict the snapshots of the amplitudes  $x_i$ .

therein).

For instance, the indirect environmental coupling plays a crucial role in facilitating complex collective dynamics such as decoherence, co-ordinated rhythms in biological systems [62] and quorum sensing [66, 67, 76, 77]. Our studies show that such a type of coupling along with a nonlocal coupling leads to a rich variety of complex collective behaviour like different types of chimeras, solitary state, and complete synchronized state reported in the literature using different coupling architectures. These are necessary and important complements to the current knowledge on the collective behaviors due to the dynamic environmental coupling. In addition, such a coupling facilitates a new type of interesting chimera, namely chimera at the phase-flip bifurcation/transition of the ensemble of oscillators for appropriate coupling strengths.

The plan of the paper is as follows. In Sec. II, the emergence of chimera at the phase-flip transition and the conventional chimera from the nonlocally coupled Rössler oscillators with a common dynamic environment will be discussed. Similarly, in Sec. III, we corroborate the generic nature of the results in the nonlocally coupled Stuart-Landau oscillators with a common dynamic environment. Finally, in Sec. IV, we provide the summary and conclusion. We present the existence of clusters with phase-flip transition, which is a special case of classical spatial chaos for different sets of initial conditions in Appendix-A, the results of phase-flip transition between two coupled oscillators in Appendix-B and also discuss the emergence of bistability among them in Appendix-C.

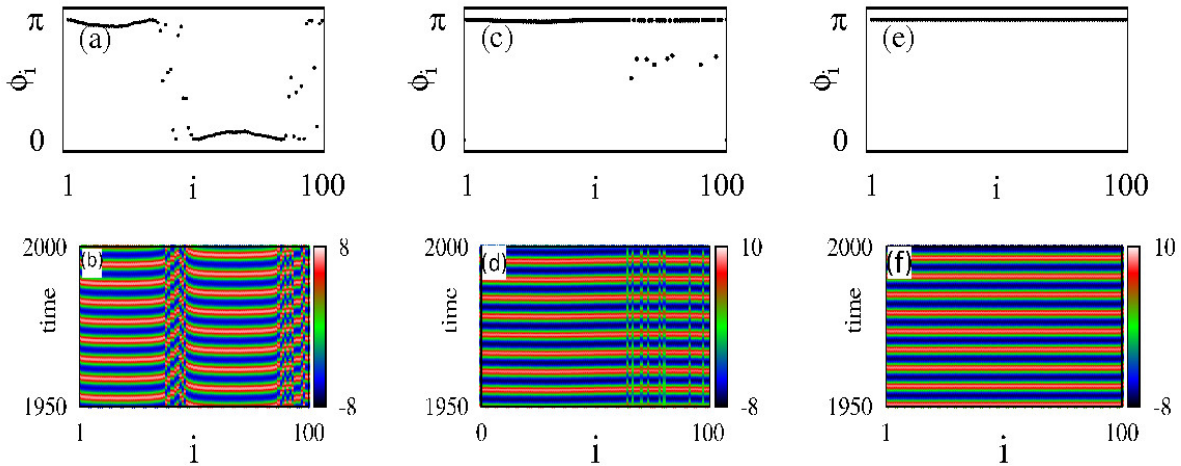


Figure 3: (Color online) Snapshots of the instantaneous phases  $\phi_i$  (left column) and the space-time evolution (right column) of the ensemble of Rössler oscillators with  $q = 0.4$  for the coupling radius  $r = 0.3$  of the nonlocal coupling and for different values of the strength of the nonlocal coupling (a)-(b)  $\varepsilon = 0.03$ , (c)-(d)  $\varepsilon = 0.051$  and (e)-(f)  $\varepsilon = 0.1$ . The values of the other parameter are the same as in Fig. 1(c).

## 2. Nonlocally coupled Rössler oscillators with common dynamic environment

We consider an ensemble of nonlocally coupled identical chaotic Rössler oscillators interacting through a common dynamic environment represented as

$$\dot{x}_i = -y_i - z_i + \frac{\varepsilon}{2P} \sum_{j=i-P}^{j=i+P} (x_j - x_i), \quad (1a)$$

$$\dot{y}_i = x_i + ay_i, \quad (1b)$$

$$\dot{z}_i = b + z_i(x_i - c) + kw_i, \quad (1c)$$

$$\dot{w}_i = -\alpha w_i + 0.5z_i - \eta(w_i - \frac{q}{N} \sum_{j=1}^N w_j), \quad (1d)$$

$$i = 1, 2, \dots, N$$

where  $\alpha = 1, a = 0.165, b = 0.4$  and  $c = 8.5$  are the system parameters and the number of oscillators is fixed as  $N = 100$  throughout the manuscript. The evolution of every individual oscillator is governed by a direct and an indirect coupling, namely a nonlocal coupling and an environmental coupling, respectively.  $P \in (1, N/2)$  quantifies the number of nearest neighbors of any oscillator in the ring with a coupling radius  $r = \frac{P}{N}$ , which provides the measure of nonlocal coupling.  $\varepsilon$  is the coupling strength of the nonlocal coupling. We have employed the same environmental coupling used to induce phase-flip transition between two coupled dynamical systems in Ref. [64] In this coupling, there are agents interacting with each other in a common dynamic environment and the  $i$ th individual oscillator in the ensemble interacts directly with the  $i$ th agent of the environment with a coupling strength  $k$ . Specifically, the evolution equation for each agent  $w_i$  is given by Eq. f(1d), where  $\eta$  is a diffusion constant and  $q$  is the strength of the mean field interaction of all the agents. Since the effect of environmental factors on the oscillators are relatively feeble compared to the interactions among the oscillators, the agents from the common environment usually interact strongly with large coupling strengths in order to have an appreciable influence on the oscillators. Hence, the coupling strength  $k$  is usually large as adopted in Ref. [64] to realize the phase-flip bifurcations. Such environmental couplings play a vital role in biochemical reactions at the cellular level [64, 73, 76, 78]. The dynamic

environmental coupling facilitates the onset of the phase-flip transition among the oscillator ensemble even in the absence of the nonlocal coupling, whereas the nonlocal coupling induces asynchronous state at the phase-flip transition among the out-of-phase synchronized coherent domains. Consequently, one is lead to the onset of coexisting coherent and incoherent domains corroborating the emergence of an interesting new type of chimera state, namely chimera at the phase-flip transition.

In order to realize the above phenomenon, first we will examine the emerging dynamics of the ensemble of Rössler oscillators (1) due to environmental coupling as a function of the strength of the mean field interaction  $q$ . For this the strength of the nonlocal diffusive coupling  $\varepsilon$  is fixed as  $\varepsilon = 0.0$ . The coupling strength between the agents and the oscillators is fixed as  $k = 25$ , while the diffusion constant  $\eta$  as  $\eta = 2.0$ , as in Ref. [64], throughout this section. We have used the Runge-Kutta fourth order integration scheme with an integration time step of 0.01 to solve the dynamical equations. One can also use smaller values of integration time step but which we find only increases the transient times to observe the stable dynamical states and do not alter our results. Therefore we fix the time step as 0.01 in our entire analysis. In our analysis, we have discarded  $4 \times 10^5$  time steps as transients to ensure that the observed dynamical behaviors are steady state dynamics and not transients. Snapshots of the instantaneous phases of all the oscillators in the ensemble along with their spatio-temporal evolution are shown in Fig. 1 for three different values of the strength of the mean field coupling  $q$ . Random initial conditions uniformly distributed between  $-1$  to  $1$  are chosen among the ensemble of Rössler oscillators. The oscillators in the ensemble display an asynchronous state both in the snapshot of their instantaneous phases (see Fig. 1(a)) and in their space-time plot (see Fig. 1(b)) for  $q = 0.02$ . Upon increasing the strength of the mean field coupling, the oscillators get randomly segregated into an in-phase and anti-phase synchronized state as shown in Figs. 1(c) and 1(d) for  $q = 0.4$ , displaying the existence of *PFC*, which is a special case of classical spatial chaos [16, 17, 61]. (We also point out in Appendix-A that clusters with phase-flip transition arise not essentially due to specific choice of initial conditions but more because of environmental coupling by illustrating that these states emerge for widely different initial conditions). It is also to be noted that even though Figs. 1(c) has some resemblance to Fig. 2 (e) in Ref. [16], both are dynamically different. Two coherent regimes which are split into simply a lower branch and an upper branch interspersed by an incoherent regime is depicted in Fig. 2(e) of Ref. [16]. In contrast, our results in Fig. 1(c) display not simply two coherent regimes splitting into lower and upper branches but two out-of-phase synchronized coherent regimes (branches) with a relative phase difference of  $\pi$ , resembling phase-flip bifurcation/transition in an ensemble of oscillators, interspersed by an incoherent regime. For further larger value of  $q$ , all the oscillators evolve in synchrony as depicted in Figs. 1(e) and 1(f) for  $q = 1.0$ .

Now we will unravel the effect of the nonlocal coupling on the asynchronous state and the *PFC* observed for the strengths of the mean field coupling  $q = 0.02$  and  $q = 0.4$  in Figs. 1(a, b) and 1(c, d) respectively. To start with, we will consider the asynchronous state for  $q = 0.02$  depicted in Figs. 1(a)-1(b) and increase the strength of the nonlocal coupling  $\varepsilon$ . Snapshots of the instantaneous phases of all the oscillators along with their spatio-temporal evolution are illustrated in Figs. 2 for different values of  $\varepsilon$ . The radius of the nonlocal coupling is fixed as  $r = 0.3$ . Even for a very low value of the strength of the nonlocal coupling, the oscillators in the ensemble splits into coherent and incoherent domains as shown in Figs. 2(a) and 2(b) for  $\varepsilon = 0.01$  elucidating the existence of conventional chimera (*CH-I*). It is to be noted that the phases of the asynchronous oscillators for  $\varepsilon = 0$  are distributed between  $0$  and  $\pi$  (see Fig. 1(a)), whereas the phases of the oscillators in the coherent and incoherent domains comprising the chimera state for a finite value of  $\varepsilon$  is shifted towards  $\pi$  (see Fig. 2(a)) indicating the tendency towards an entanglement of their phases. The ensemble of oscillators evolve in coherence (*CO*) as depicted in the snapshot and space-time plots in Figs. 2(c) and 2(d), respectively, for  $\varepsilon = 0.02$ , where the coherent evolution of the oscillators is evident from the inset of Fig. 2(c). The oscillators evolve in complete synchrony (*CS*) (see the inset of Fig. 2(e)) for a further larger value of the strength of the nonlocal coupling as shown in Figs. 2(e) and 2(f) for  $\varepsilon = 0.05$ .

Next, we will illustrate the effect of the nonlocal coupling on the *PFC* state in Fig. 1(c)-1(d) induced by the mean field coupling with  $q = 0.4$ . Snapshots of the instantaneous phases of all the oscillators along with their spatio-temporal evolution are illustrated in Figs. 3 for different values of  $\varepsilon$ . Now, the oscillators are clearly segregated into two coherent domains exhibiting out-of-phase synchronized oscillations with each other interspersed by a domain of asynchronous oscillators at the onset of the phase-flip transition among

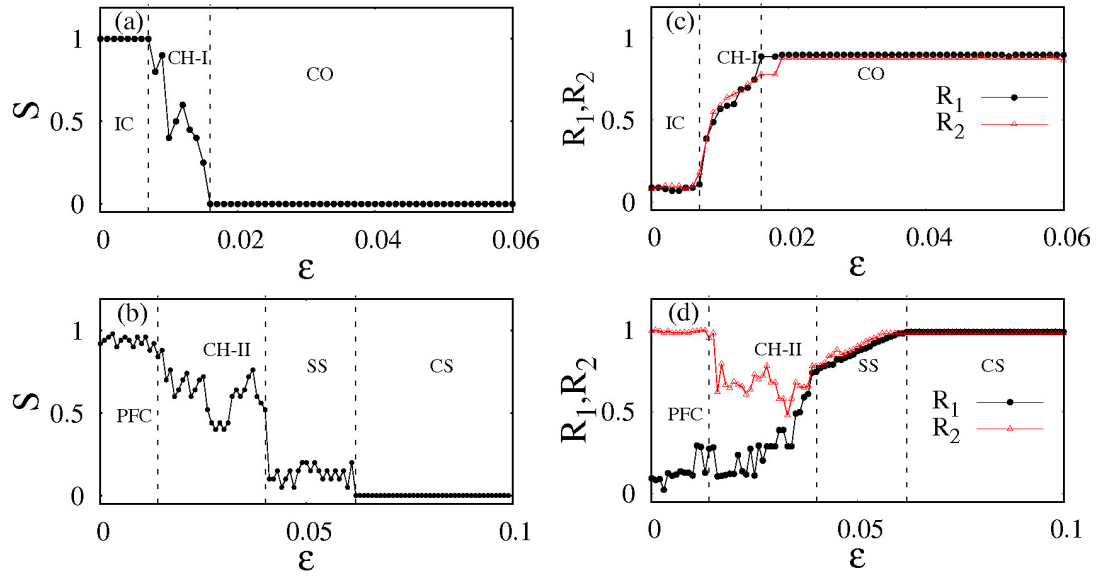


Figure 4: (Color online) The strength of incoherence  $S$  ((a)-(b)) and Kuramoto order parameter  $R_1, R_2$  ((c)-(d)) as a function of the nonlocal coupling strength  $\varepsilon$  for (a),(c)  $q = 0.02$  and (b),(d)  $q = 0.4$  characterizing the dynamical transitions in Fig. 2 and Fig. 3, respectively.

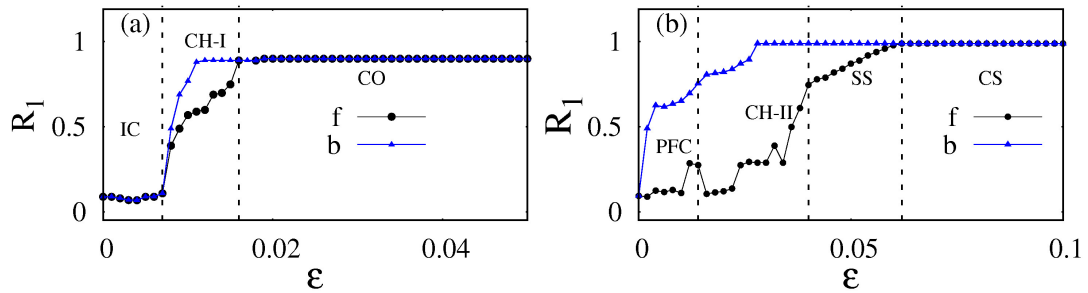


Figure 5: (Color online) Kuramoto order parameter  $R_1$  for both the forward (represented by the line 'f' connected by filled circles) and the backward (represented by the line 'b' connected by filled triangles) scanning of the nonlocal coupling strength  $\varepsilon$  for (a)  $q = 0.02$  and (b)  $q = 0.4$  depicting hysteresis in their dynamical transitions.

the oscillators as shown in Fig. 3(a) for  $\varepsilon = 0.03$ . Thus the coexisting out-of-phase synchronized coherent domains and the incoherent domain in between the coherent domains (see also Fig 3(b)) constitute an interesting new type of chimera state, namely, chimera at the phase-flip transition (*CH-II*). It is to be noted that Figs. 3(a, b) have close resemblance to Fig. 2 (d) of Ref. [16] and Fig. 4(b) of Ref. [17].

Further, we have also identified the existence of imperfectly synchronized states illustrated in Figs. 3(c)-3(d) for  $\varepsilon = 0.051$ . The imperfect synchronized states are also called solitary states, which refer to excursions of a small number of oscillators away from synchronized group [37, 38, 39, 40, 41, 42]. Thus a finite nonlocal coupling is necessary to induce the chimera at the phase-flip transition and the solitary state in addition to the common environmental coupling. It is clear that either the common environmental coupling or the nonlocal coupling alone cannot give rise to these states. Finally, the ensemble of oscillators evolve synchronously for further increase in the strength of the nonlocal coupling as shown in Figs. 3(e)-3(f) for  $\varepsilon = 0.1$ .

### 2.1. Quantification measures to characterize the chimera states

Recently a quantitative measure, namely, the strength of incoherence  $S$  [43] was introduced, to distinguish various collective dynamical states, as

$$S = 1 - \frac{\sum_{m=1}^M s_m}{M}, \quad s_m = \Theta(\delta - \sigma_l(m)), \quad (2)$$

where  $\Theta(\cdot)$  is the Heaviside step function, and  $\delta$  is a predefined threshold chosen as a certain percentage value of the difference between the upper/lower bounds,  $x_{l,i_{max}}/x_{l,i_{min}}$ .  $M$  is the number of bins of equal size  $n = N/M$ . The local standard deviation  $\sigma_l(m)$  is introduced as

$$\sigma_l(m) = \left\langle \sqrt{\frac{1}{n} \sum_{j=n(m-1)+1}^{mn} [z_{l,j} - \langle z_{l,m} \rangle]^2} \right\rangle_t, \quad (3)$$

$m = 1, 2, \dots, M$ ,

where  $z_{l,i} = x_{l,i} - x_{l,i+1}$ ,  $l = 1, 2, \dots, d$ ,  $d$  is the dimension of the individual unit in the ensemble,  $i = 1, 2, \dots, N$ ,  $\langle z_{l,m} \rangle = \frac{1}{n} \sum_{j=n(m-1)+1}^{mn} z_{l,j}(t)$ , and  $\langle \cdot \rangle_t$  denotes the time average. When  $\sigma_l(m)$  is less than  $\delta$ ,  $s_m = 1$ , otherwise  $s_m = 0$ .

In the incoherent domain, the local standard deviation  $\sigma_l(m)$  has some finite value greater than  $\delta$  and hence  $s_m = 0, \forall m$ . Hence, the strength of incoherence  $S$  acquire unit value for the incoherent domain. On the other hand, in the coherent domain, the standard deviation  $\sigma_l(m)$  is always zero and hence  $s_m = 1, \forall m$ , resulting in the null value of  $S$  ( $m$  in the present case is chosen as  $m = 20$ ). The strength of incoherence  $S$  will have intermediate values between zero and one,  $0 < S < 1$  for the chimera states as they are characterized by coexisting coherent and incoherent domains. The strength of the incoherence  $S$  is depicted in Fig. 4 for the mean field interactions  $q$  corresponding to Figs. 2 and 3 as a function of the nonlocal coupling  $\varepsilon$ . The unit value of  $S$  in the range of  $\varepsilon \in (0, 0.008)$  in Fig. 4(a) for  $q = 0.02$  indicates that the coupled oscillators evolve in asynchrony, whereas the intermediate values between zero and unity for  $\varepsilon \in (0.008, 0.016)$  corroborate the coexistence of both coherent and incoherent domains characterizing the existence of chimera states. For  $\varepsilon > 0.016$ , the null value of the strength of the incoherence confirms the synchronous evolution of the coupled oscillators. Upon increasing the strength of the mean field interaction to  $q = 0.4$ , the spread of the chimera state is extended to a larger range of  $\varepsilon \in (0.016, 0.041)$  as confirmed by the intermediate values of  $S$  in Fig. 4(b). Chimera state is preceded by *PFC* in the range of  $\varepsilon \in (0.0, 0.016)$  as indicated by the value of  $S$  close to unity as there are out-of-phase synchronized and asynchronous oscillators in all the  $m$  domains. Further, the value of  $S$  close to zero in the range of  $\varepsilon \in (0.041, 0.061)$  characterizes the existence of solitary state with a few asynchronous oscillators in the bins. Synchronous state for  $\varepsilon > 0.061$  is shown by the null values of  $S$  in Fig. 4(b). In order to confirm the above states further, we also estimated the Kuramoto order parameters  $R_1, R_2$  defined by [74, 75]

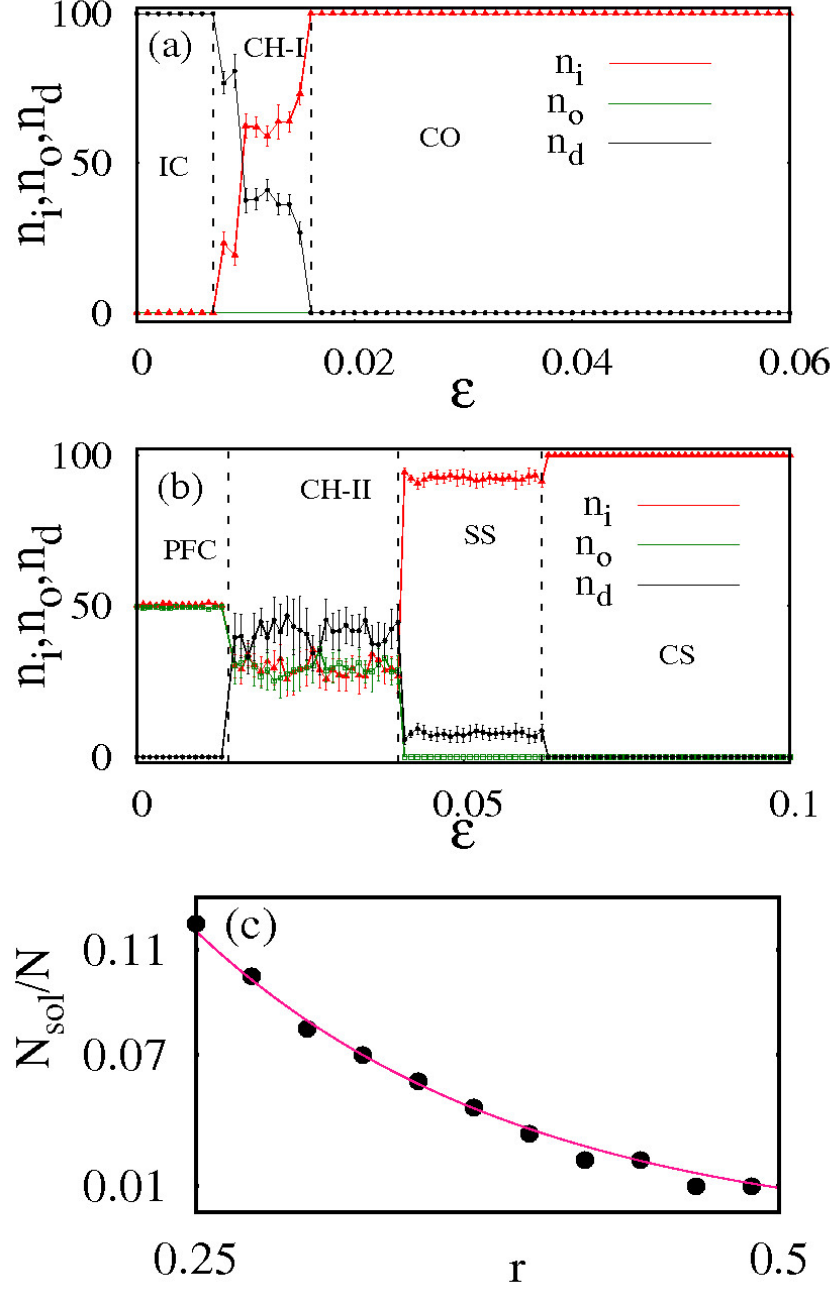


Figure 6: (Color online) Number of oscillators exhibiting in-phase oscillations  $n_i$ , out-of-phase oscillations  $n_o$  and desynchronized state  $n_d$  as a function of the strength of the nonlocal coupling for different values of the coupling radius (a)  $q = 0.02$  and (b)  $q = 0.4$  characterizing the dynamical transitions in Fig. 2 and Fig. 3, respectively, with error bars indicated. (c) The solitary fraction, namely the ratio of the number of desynchronized oscillators (solitary oscillators)  $N_{sol}$  to the total number of the oscillators  $N$  as a function of the coupling radius  $r$ , displays an exponential decay.



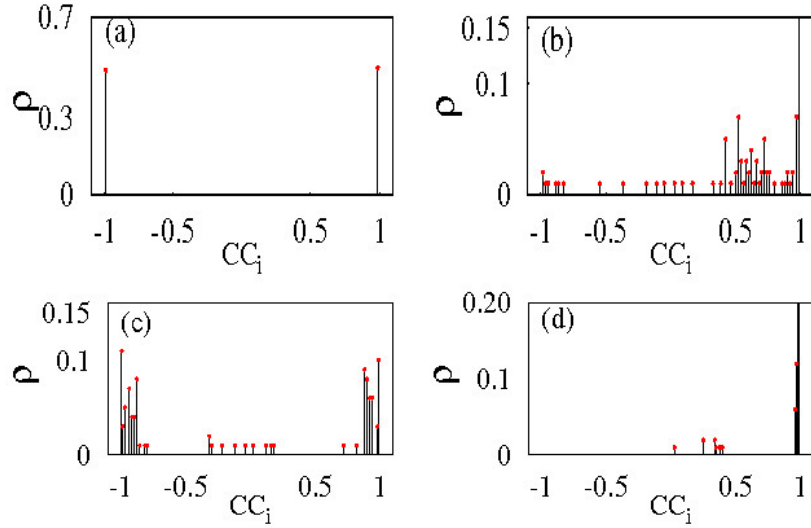


Figure 7: (Color online) Probability distribution of correlation coefficient for different collective dynamical states in the ensembles of Rössler oscillators: (a) phase flip chimera ( $\epsilon = 0.0, q = 0.4$ ), (b) chimera I ( $\epsilon = 0.01, q = 0.02$ ), (c) chimera II ( $\epsilon = 0.03, q = 0.4$ ), (d) solitary states ( $\epsilon = 0.051, q = 0.4$ ).

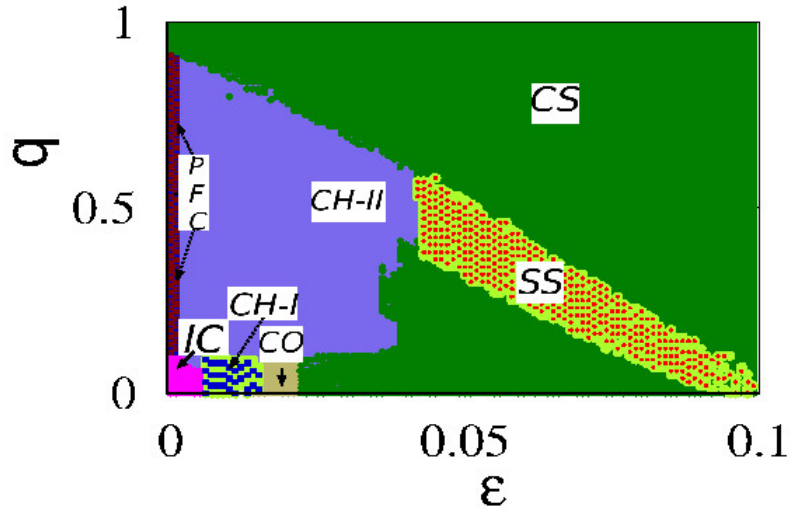


Figure 8: (Color online) Two parameter phase diagram depicting the collective dynamical states of nonlocally coupled Rössler oscillators with a common dynamic  $q$  environment as a function of the strength of the nonlocal coupling  $\epsilon \in (0, 0.1)$  and the strength of the mean field coupling  $q \in (0, 1)$ . The parameter regions marked as  $IC$ ,  $PFC$ ,  $CH-I$ ,  $CH-II$ ,  $SS$ ,  $CO$ , and  $CS$  correspond to the desynchronized state,  $PFC$ , conventional chimera, chimera at the phase-flip transition, solitary state, phase synchronized state and complete synchronized state, respectively.

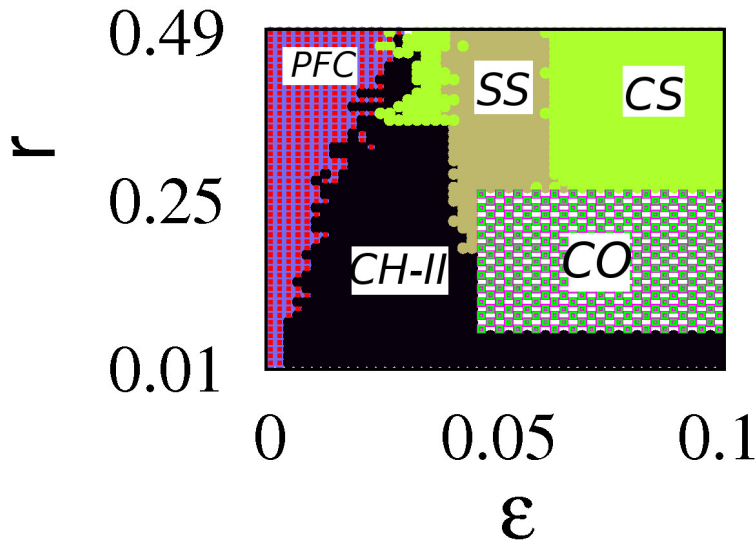


Figure 9: (Color online) (a) Two-phase diagram as a function of the strength of the nonlocal coupling  $\varepsilon \in (0, 0.1)$  and the coupling radius  $r \in (0.01, 0.49)$  in an array of nonlocally coupled Rössler oscillators under common environmental coupling, demarcating different collective dynamical regimes.

$$R_n = \left\langle \frac{1}{N} \left| \sum_{j=1}^N e^{in\theta_j} \right| \right\rangle_t, \quad \text{where } n = 1, 2, \quad (4)$$

Note that here  $R_1$  and  $R_2$  correspond to the order parameters in Eq.(4). Here  $R_1$  corresponds to in-phase synchronization and  $R_2$  corresponds to out-of-phase synchronization. In particular, values of both  $R_1$  and  $R_2$  are required to characterize the *PFC*.  $R_1$  will acquire null value for out-of-phase synchronized oscillators whereas  $R_2$  will acquire unit value for the same set of out-of-phase synchronized oscillators as  $R_2 = e^{2i\theta}$ . The coupled system exhibits an incoherent state when the oscillator phases are uniformly distributed so that  $R_1 \approx R_2 \approx 0$  and coherent state when their phases are entrained,  $R_1 \approx R_2 \approx 1$ . The order parameter takes intermediate values,  $0 \leq R_1, R_2 \leq 1$ , for chimera state. The order parameters acquire values 0 and 1 for *PFC* as in the case of two clusters which are out-of-phase with each other (See. Figs 4(d)). The Kuramoto order parameter, corresponding to Figs. 4(a-b), depicted in Figs. 4(c-d) again confirm the transitions shown by the strength of incoherence. The strength of incoherence and the Kuramoto order parameters in Figs. 4(a-b) and 4(c-d), respectively, elucidate the transitions among the different states are second order transitions as there is a smooth transition from one state to the other. In addition, the order parameter  $R_1$  is also depicted for both the forward scanning (represented by the line ‘f’ connected by filled circles) and the backward scanning (represented by the line ‘b’ connected by filled triangles), starting from the same final conditions at the end of forward scanning, of the coupling strength  $\varepsilon$  in Figs. 5(a)-(b) for  $q = 0.02$  and  $0.4$ , respectively, illustrating the existence of hysteresis in their dynamical transitions.

We have also quantified the emergent dynamical states in terms of the number of oscillators exhibiting in-phase oscillations, anti-phase oscillations and desynchronized state as  $n_i, n_o$  and  $n_d$  to characterize the distinct dynamical behaviors observed as a function of the system parameters. This is carried out by means of the cross-correlation co-efficient (*CC*) defined as

$$CC_i = \frac{\langle (x_r(t) - \langle x_r(t) \rangle) (x_i(t + \Delta t) - \langle x_i(t) \rangle) \rangle_t}{\sqrt{\langle (x_r(t) - \langle x_r(t) \rangle)^2 \rangle_t \langle (x_i(t) - \langle x_i(t) \rangle)^2 \rangle_t}}, \quad (5)$$

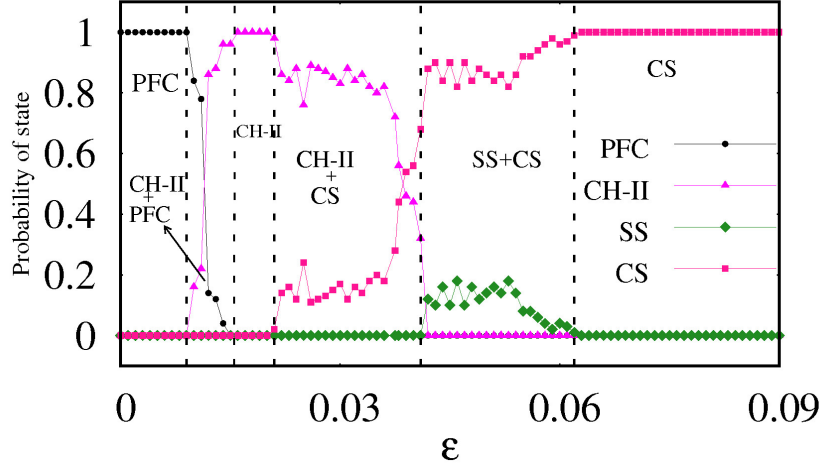


Figure 10: (Color online) The probability of occurrence of clusters with phase-flip transition (*PFC*), chimera at the phase-flip transition (*CH – II*), solitary state (*SS*) and complete synchronized state (*CS*) out of a set of 100 different realizations using 100 different initial conditions for each oscillators as a function of the nonlocal coupling strength  $\varepsilon$  for  $q = 0.4$ ,  $r = 0.3$  and  $N = 100$ .

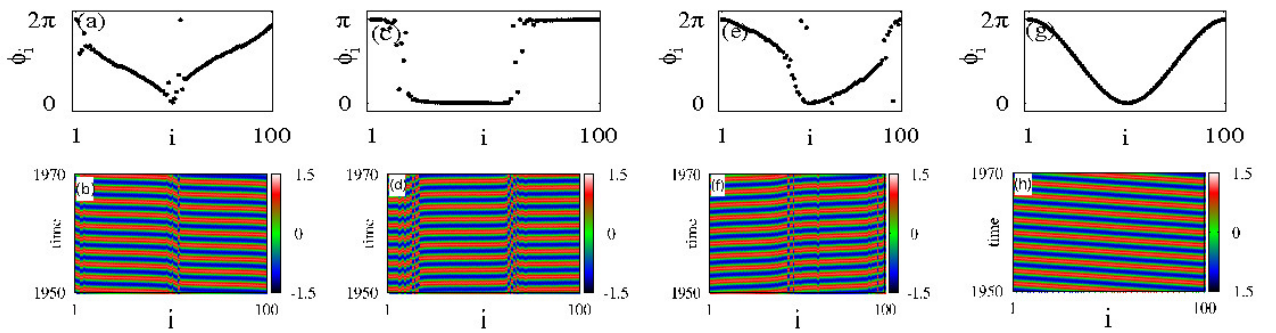


Figure 11: (Color online) Snapshots of the instantaneous phases  $\phi_i$  (top row) and the space-time evolution (bottom row) of the ensemble of Stuart-Landau oscillators for the coupling radius  $r = 0.3$  and for different values of the strength of the nonlocal coupling (a)-(b)  $q = 0.4$ ,  $\varepsilon = 0.04$ , (c)-(d)  $q = 0.8$ ,  $\varepsilon = 0.04$ , (e)-(f)  $q = 0.8$ ,  $\varepsilon = 0.08$ , and (g)-(h)  $q = 0.8$ ,  $\varepsilon = 0.12$ . The values of the other parameter are  $\omega = 10$ ,  $k = 25$ ,  $k_1 = 0.5$ ,  $q = 0.8$  and  $\eta = 10$ .

where  $i = 1, 2, \dots, N$  and  $r \neq i$ ,  $\langle \cdot \rangle_t$  represents the time average,  $\Delta t$  is the time shift, and  $x_r$  is the reference oscillator chosen either from the in-phase (complete synchronized/coherent) or anti-phase synchronized domain. Thus for in-phase synchronized oscillators the correlation coefficient is characterized by  $+1$ , whereas for anti-phase synchronized oscillators  $CC_i$  acquires the value  $-1$ . The desynchronized oscillators are characterized by intermediate values between  $\pm 1$ . The number of  $+1$ ,  $-1$  and the intermediate values between them acquired by  $CC_i$  provide the estimate of the number of in-phase synchronized oscillators  $n_i$ , the number of anti-phase synchronized oscillators  $n_o$  and the number of desynchronized oscillators  $n_d$ , respectively.

The numbers of oscillators in each of the above states, calculated for 100 different realizations, are shown in Figs. 6(a) and 6(b) for  $q = 0.02$  and  $q = 0.4$ , respectively, along with the error bars as a function of the strength of the nonlocal coupling  $\varepsilon$ . The number of desynchronized oscillators  $n_d$  equal to the total number of oscillators in the ensemble in the range of  $\varepsilon \in (0, 0.008)$  in Fig. 6(a) confirms asynchronous evolution of the ensemble of oscillators. The finite number of in-phase synchronized and desynchronized oscillators in the range of  $\varepsilon \in (0.008, 0.018)$  elucidates the conventional chimera. For  $\varepsilon > 0.018$ , the number of in-phase synchronized oscillators equal to the total number of oscillators  $N$  corroborates the in-phase synchronous evolution of the ensemble of oscillators. It is also to be noted that the number of anti-phase synchronized oscillators remain at null value for the entire range of  $\varepsilon$  in Fig. 6(a).

In Fig. 6(b), the number of oscillators exhibiting in-phase and anti-phase oscillations are almost equal in number in the range of  $\varepsilon \in (0, 0.016)$  corresponding to the existence of *PFC* without any oscillators with random phases. In the range of  $\varepsilon \in (0.016, 0.041)$ , the number of desynchronized oscillators  $n_d$  increases and almost equal to  $n_i$  and  $n_o$  corroborating the coexistence of anti-phase synchronized coherent domains along with the desynchronized domains, that is chimera at the phase-flip transition. Beyond  $\varepsilon = 0.041$ , there exists almost completely synchronized oscillators as indicated by  $n_i$  close to  $N = 100$  coexisting along with a few desynchronized oscillators confirming the existence of solitary states up to  $\varepsilon = 0.062$ . The values of  $n_i$  attain unity for  $\varepsilon > 0.062$  elucidating the emergence of completely synchronized state.

In Fig. 6(c), we have depicted the solitary fraction, namely the ratio of number of desynchronized oscillators  $N_{sol}$  to the total number of oscillators  $N$  in the ensemble to characterize the solitary state. We have fixed the value of the coupling strength  $\varepsilon = 0.051$  and vary the coupling radius  $r$ . It is evident that the average number of oscillators excusing away from the synchronized state, shown by the line connecting filled circles, representing the solitary state decreases exponentially upon increasing the coupling radius. The dotted line corresponds to the exponential fit. As the coupling radius is increased to include more number of nearest neighbors, the tendency of synchronization among them also increases for a given coupling strength resulting in more number of synchronized oscillators and a corresponding decrease in the number of desynchronized oscillators thereby leading to an exponential decay of the average number of oscillators excusing away from the synchronized state. It may also be noted that when the coupling radius approaches the global coupling limit the number of desynchronized oscillators (solitary oscillators) in the solitary state decreases while for an intermediate value of the coupling radius ( $r = 0.25$ ) the solitary oscillators are large in number.

Further, we have also estimated the probability distribution of the correlation coefficient  $\rho = \text{pbt}(CC_i)$  to characterize the different types of chimeras and solitary state. The probability distribution of the correlation coefficient corresponding to the different collective dynamical states in the ensemble of Rössler oscillators is shown in Fig. 7. The distribution of the correlation coefficient in Fig. 7(a) is centered only at  $+1$  and  $-1$  for  $\varepsilon = 0.0$  and  $q = 0.4$  elucidating the *PFC* with only in-phase and anti-phase synchronized states. The distribution centered about  $+1$  with finite distributions between  $\pm 1$  in Fig. 7(b) for  $\varepsilon = 0.01$  and  $q = 0.02$  characterizes the conventional chimera (*CH - I*) (see Fig. 2(b)) coexisting with in-phase synchronized domain and desynchronized domains. The probability distribution localized at both  $+1$  and  $-1$  along with finite distribution between them in Fig. 7(c) confirms the chimera at the phase-flip transition (*CH - II*) for  $\varepsilon = 0.03$  and  $q = 0.4$  as it is characterized by out-of-phase synchronized coherent domains interspersed by asynchronous incoherent domain. The maximal probability at  $+1$  with a few intermediate distributions between  $\pm 1$  characterizes the solitary state in Fig. 7(d) for  $\varepsilon = 0.051$  and  $q = 0.4$ .

The robustness of the observed dynamical transitions as a function of the strength of the nonlocal coupling  $\varepsilon \in (0, 0.1)$  and that of the mean field coupling  $q \in (0, 1)$  is elucidated in the two-phase diagram shown in Fig. 8. The different dynamical regimes are demarcated using the strength of incoherence  $S$ ,

number of oscillators exhibiting in-phase oscillations  $n_i$ , out-of-phase oscillations  $n_o$  and desynchronized state  $n_d$ . The parameter space corresponding to the desynchronized state is indicated as *IC* in the range of  $\varepsilon \in (0, 0.005)$  and  $q \in (0, 0.1)$ . The parameter spaces marked as *PFC*, *CH-I* and *CH-II* correspond to the *PFC*, conventional chimera and the chimera at the phase-flip transition, respectively. The parameter regime corresponding to the phase synchronization is represented by *CO* while the parameter spaces indicated by *SS* and *CS* correspond to the solitary state and completely synchronized state, respectively. It is also clear from the two-parameter phase diagram that a set of finite values of  $\varepsilon$  and  $q$  is necessary to observe the reported new type of chimera, namely the chimera at the phase-flip transition.

We have also depicted another two-phase diagram as a function of the strength of the nonlocal coupling  $\varepsilon \in (0, 0.1)$  and the coupling radius  $r \in (0.01, 0.49)$  in Fig. 9 to illustrate the effect of the coupling radius  $r$ . The parameter regimes corresponding to the *PFC*, chimera at the phase-flip transition, solitary state, in-phase synchronized state (coherent state) and completely synchronized state are indicated by *PFC*, *CH-II*, *SS*, *CO* and *CS*, respectively. It is also to be noted that as the radius of the nonlocal coupling increases, the spread of the *PFC* also increases as a function of the coupling strength  $\varepsilon$ . On contrary, smaller values of coupling radius  $r$  favours the emergence of chimera at the phase-flip transition to a larger range of  $\varepsilon$ . It is evident from Fig. 9 that as the radius of the nonlocal coupling is decreased, the spread of the chimera at the phase-flip transition increases as a function of  $\varepsilon$ .

## 2.2. Multistability

In order to elucidate the multistability of the observed dynamical behaviors, we have estimated the probabilities of the *PFC*, chimera at the phase-flip transition, solitary state and complete synchronized state out of a set of 100 different realizations using 100 random initial conditions, where each of the oscillators is distributed between 1 and  $-1$ . The parameter values are fixed as  $q = 0.4$  and  $r = 0.3$  and the probability distribution is depicted in Fig. 10 as a function of the strength of the nonlocal coupling. The dynamical states, namely *PFC*, chimera at the phase-flip transition, solitary state and complete synchronized state, are represented by lines connecting filled circles, filled triangles, filled diamonds, and filled squares, respectively. The probability of the *PFC* is unity in the range of  $\varepsilon \in (0, 0.01)$  confirming that the *PFC* is the only collective dynamical behavior observed in this range of  $\varepsilon$ . *PFC* and chimera at the phase-flip transition coexist in the range of  $\varepsilon \in [0.01, 0.015)$  illustrating multistability between them. Chimera at the phase-flip transition alone exists in the range of  $\varepsilon \in [0.015, 0.02)$ , while it coexists with the complete synchronized state in the range of  $\varepsilon \in [0.02, 0.041)$ . Further, the complete synchronized state coexists with the solitary state in the range of  $\varepsilon \in [0.041, 0.064)$ . Beyond  $\varepsilon = 0.064$ , one finds that the complete synchronized state is monostable.

## 3. Nonlocally coupled Stuart-Landau oscillators with common dynamic environment

In this section, we demonstrate the emergence of chimera states at the phase-flip transition with two out-of-phase synchronized coherent domains characterizing phase-flip transition interspersed by an asynchronous incoherent domain in an ensemble of identical Stuart-Landau oscillators with both nonlocal and dynamic environmental couplings. The corresponding evolution equations are represented as

$$\dot{x}_i = (1 - (x_i^2 + y_i^2))x_i - \omega y_i + \frac{\varepsilon}{2P} \sum_{j=i-P}^{j=i+P} (x_j - x_i), \quad (6a)$$

$$\dot{y}_i = (1 - (x_i^2 + y_i^2))y_i + \omega x_i + k w_i, \quad (6b)$$

$$\dot{w}_i = -w_i + k_1 y_i - \eta \left( w_i - \frac{q}{N} \sum_{j=1}^N w_j \right), \quad (6c)$$

$$i = 1, 2, \dots, N.$$

where  $\omega = 10$ , and  $k_1 = 0.5$  are the system parameters. The agents in the common environment interact with the oscillators with the strength  $k = 25$  and the diffusion coefficient  $\eta$  is fixed as  $\eta = 10$ . In the absence of the

nonlocal coupling, all the oscillators evolve in asynchrony below a threshold value of the mean field coupling  $q$ , above which the oscillators in the ensemble evolve in complete synchrony. The dynamic environmental coupling is incapable of inducing phase-flip transition in the ensemble of Stuart-Landau oscillators in the absence of the nonlocal coupling, whereas the same coupling has been shown to induce phase-flip transition in two coupled Stuart-Landau oscillators for  $\varepsilon = 0$  [64]. To examine the collective dynamical behaviors induced by the nonlocal coupling in the ensemble of Stuart-Landau oscillators coupled indirectly through the dynamic environment, the strength of the mean field diffusive coupling  $q$  and the strength of the nonlocal coupling  $\varepsilon$  are varied while the radius of the nonlocal coupling is fixed as  $r = 0.3$  and the total number of oscillators is fixed as  $N = 100$ . Initial conditions are chosen on the sphere  $x^2 + y^2 + w^2 = 1$ .

The snapshots of the instantaneous phases and the spatiotemporal plots of the ensemble of coupled Stuart-Landau oscillators are depicted in Fig. 11 for different values of  $q$  and  $\varepsilon$ . The oscillators in the ensemble display conventional chimera ( $CH - I$ ) for a low value of mean field diffusive coupling  $q = 0.4$  and the nonlocal coupling strength  $\varepsilon = 0.04$  (see Figs. 11(a) and 11(b)). Now, the mean field diffusive coupling is increased to  $q = 0.8$  and by varying the strength of the nonlocal coupling, the ensemble of oscillators is found to split into coherent domains exhibiting out-of-phase synchrony interspersed by an incoherent domain comprised of desynchronized oscillators. Such a state reveals the interesting new type of chimera, namely, chimera at the phase-flip transition. Such a chimera ( $CH - II$ ) is shown in the snapshot of the instantaneous phases (see Fig. 11(c)) of the oscillators and their space-time plot (see Fig. 11(d)) for  $\varepsilon = 0.04$ . Further increase in the strength of the nonlocal coupling leads to the emergence of solitary states where random oscillators hop away from the synchronized/coherent oscillators as illustrated in Figs. 11(e) and 11(f) for  $\varepsilon = 0.08$ . Finally, a travelling wave pattern emerges from the ensemble of oscillators for large coupling strengths (see Figs. 11(g) and 11(h) for  $\varepsilon = 0.12$ ).

The strength of incoherence  $S$  is depicted in Fig. 12(a) to characterize the observed collective dynamical behavior in Fig. 11. We have estimated the strength of incoherence for  $q = 0.8$  and hence one can observe only the chimera at the phase-flip transition, solitary state and complete synchronized state as a function of  $\varepsilon$ . The unit value of the strength of incoherence  $S$  in the range of  $\varepsilon \in (0, 0.01)$  elucidates the asynchronous evolution of the coupled Stuart-Landau oscillators. Chimera at the phase-flip transition is observed in the range of  $\varepsilon \in [0.01, 0.066]$  as is indicated by the value of  $S$  less than unity but greater than  $S = 0.5$  attributing to the fact that asynchronous oscillators in the incoherent domain of  $CH - II$  are large in number. Solitary state is observed in the range of  $\varepsilon \in [0.066, 0.1]$  as the value of  $S$  is rather low here corresponding to a small number of solitary oscillators. The value of the strength of incoherence  $S$  decreases smoothly in the range attributing to the fact that all the oscillators are in coherent state, and not in the completely synchronized state, other than the solitary oscillators. The null value of the strength of incoherence  $S$  for  $\varepsilon > 0.1$  corroborates the complete synchronized state. We have also depicted the solitary fraction of the ensemble of Stuart-Landau oscillators to characterize the solitary state in the inset of Fig. 12 in the range of  $\varepsilon \in [0.066, 0.1]$ . As in the case of Stuart-Landau oscillators, the number of solitary oscillators, shown by line connecting filled circles, decreases exponentially as the nonlocal coupling strength  $\varepsilon$  is increased. The dotted line corresponds to the exponential fit. It indicates that, as the coupling radius is increased to include more number of nearest neighbors, the tendency of synchronization among them is increased for a given coupling strength resulting in more number of synchronized oscillators and a corresponding decrease in the number of desynchronized oscillators thereby leading to an exponential decay of the average number of oscillators excusing away from the synchronized state. Similar scaling for solitary states is also reported in Refs. [37, 38, 39, 40, 41, 42] for a system of nonlocally coupled pendulum like oscillators and Stuart-Landau oscillators. Further, in order to confirm the existence of different collective dynamical states, we also plotted the Kuramoto order parameters  $R_1, R_2$  versus coupling strength. It also distinguishes different collective dynamical states in terms of  $R_1 = R_2 \approx 0$  if phases of oscillators are uniformly distributed,  $R_1 = R_2 \approx 1$  for travelling wave state, in the case of  $CH - II$ , the order parameter takes a values of  $0 \leq R_1, R_2 \leq 1$ . One may also note that both the strength of incoherence and the Kuramoto order parameter confirm the transition among the different states is a second order transition as there is a smooth transition from one state to another.

To characterize the different dynamical behaviors observed in the coupled Stuart-Landau oscillators, we have further depicted the probability of cross correlation  $\rho = CC_i$  in Figs. 12(c) and (d). Now, the value of

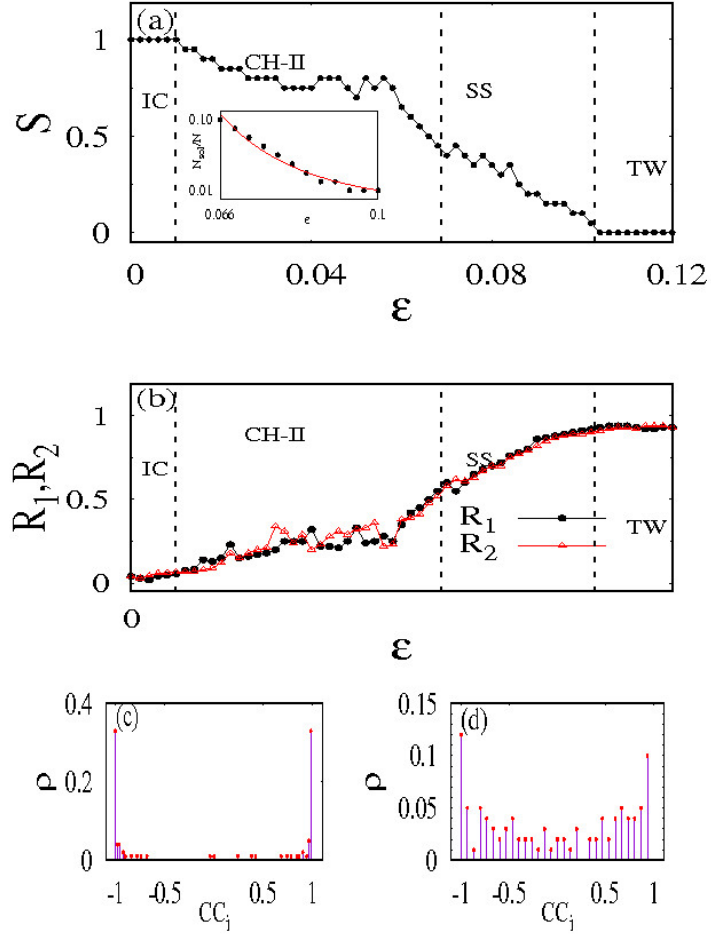


Figure 12: (Color online) (a) The strength of incoherence  $S$ , (b) Kuramoto order parameter  $R_1$ ,  $R_2$  as a function of the nonlocal coupling strength  $\epsilon$  for  $q = 0.8$  (The inset shows that  $\frac{N_{sol}}{N}$  versus  $\epsilon$ , where  $N_{sol}$  denotes number of oscillators away from synchronized group, namely the solitary fraction). Probability distribution of correlation coefficient for different collective dynamical states in the ensembles of Stuart- Landau oscillator (c) chimera II ( $q = 0.8, \epsilon = 0.04$ ), and (d) solitary states ( $q = 0.8, \epsilon = 0.08$ ).

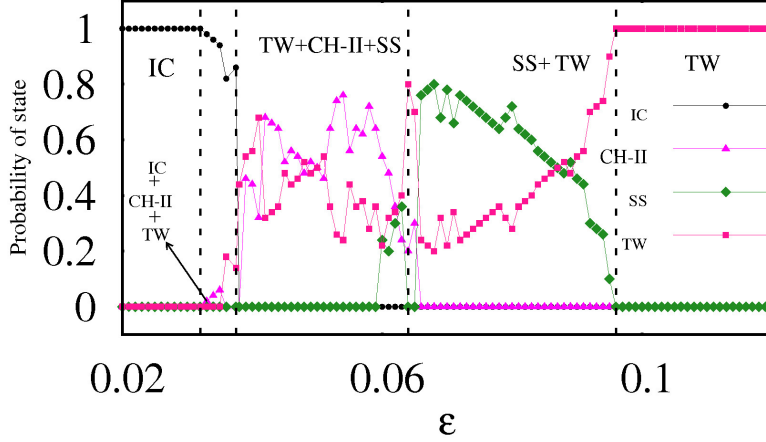


Figure 13: (Color online) The probability of occurrence of asynchronous state (*DSYC*), chimera at the phase-flip transition (*CH-II*), solitary state (*SS*) and travelling wave pattern (*TW*) as a function of the nonlocal coupling strength  $\varepsilon$  for  $q = 0.4$ ,  $r = 0.3$  and  $N = 100$  respectively.

$q$  is fixed as  $q = 0.8$  to characterize the *CH-II* state observed in Fig. 12(a). The probability distributions localized at both  $+1$  and  $-1$  along with finite distribution between them in Fig. 12(c) confirms the chimera at the phase-flip transition (*CH-II*) for  $\varepsilon = 0.04$ . It is characterized by out-of-phase synchronized coherent domain interspersed by an asynchronous incoherent domain. The maximal probability at  $+1$  with a few intermediate distributions between  $\pm 1$  characterizes the solitary state in Fig. 12(d) for  $\varepsilon = 0.08$ .

In order to elucidate the multistability nature of the observed dynamical behavior in coupled Stuart-Landau oscillators, we have estimated the probabilities of the asynchronous state, chimera at the phase-flip transition, solitary state and complete synchronized state out of 100 random initial conditions for each oscillators satisfying  $x^2 + y^2 + w^2 = 1$ . The parameter values are fixed as  $q = 0.8$  and  $r = 0.3$  and the probability distribution is depicted in Fig. 13 as a function of the strength of the nonlocal coupling. The dynamical states, namely, asynchronous state, chimera at the phase-flip transition, solitary state and travelling wave pattern are represented by line connecting filled circles, filled triangles, filled diamonds, and filled squares, respectively. Asynchronous state alone exists in the range of  $\varepsilon \in (0, 0.032)$  as indicated by the null value of the probability distributions of various collective states other than that of the asynchronous state. Chimera at the phase-flip transition (*CH-II*) and travelling wave (*TW*) coexists along with the asynchronous state in the range of  $\varepsilon \in [0.032, 0.038)$  attributing to the finite value of their probability distributions. *CH-II* and *TW* coexist in the range of  $\varepsilon \in [0.038, 0.066)$  as shown by their probabilities in Fig. 13. Further, *CH-II* and *TW* coexist along with the solitary state (*SS*) in the range of  $\varepsilon \in [0.066, 0.097)$ , whereas *TW* and *SS* exists in the range of  $\varepsilon \in [0.066, 0.097)$  demonstrating their multistable nature. For  $\varepsilon > 0.97$  travelling wave pattern alone is stable as indicated by the unit value of its probability.

For a global perspective of the emerging collective dynamics of the ensemble of nonlocally coupled Stuart-Landau oscillators with the common environmental coupling, a two-parameter phase diagram is depicted in Fig. 14 as a function of the strength of the nonlocal coupling  $\varepsilon \in (0, 1)$  and the strength of the mean field coupling among the agents  $q \in (0, 1)$ . The parameter space that results in the desynchronized state is represented by *IC* in Fig. 14. The set of parameter values that can give rise to the chimera state at the phase-flip transition, solitary state, and travelling wave patterns are marked as *CH-II*, *SS*, and *TW*, respectively, in the two-phase diagram.

### 3.1. Other initial conditions: Stuart-Landau Oscillators

Further, it is to be noted that the emergence of clusters with phase-flip transition (*PFC*) or chimera at the phase flip transition state highly relies on the nature of distribution of the initial conditions of the



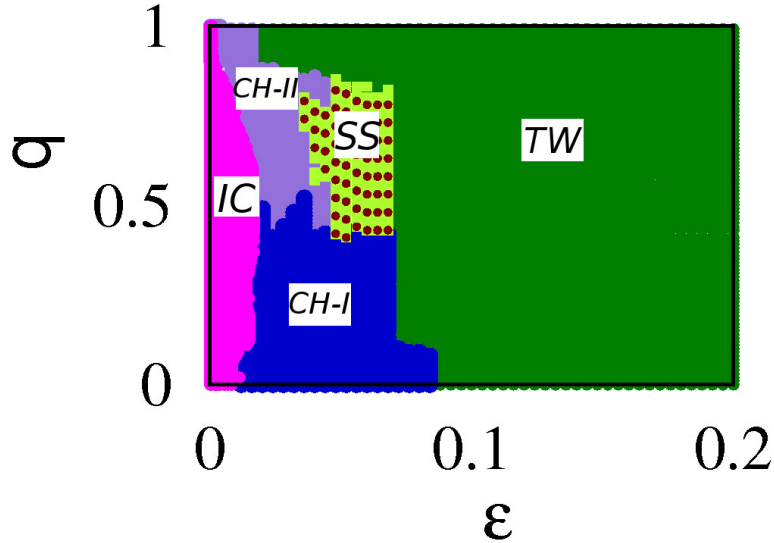


Figure 14: (Color online) Two parameter phase diagram depicting the collective dynamical states of nonlocally coupled Stuart-Landau oscillators with a common dynamic environment as a function of the strength of the nonlocal coupling  $\varepsilon \in (0, 0.2)$  and the strength of the mean field coupling  $q \in (0, 1)$ . The parameter space marked as *IC*, *CH - I*, and *TW* corresponds to the desynchronized state, chimera at phase-flip transition, and travelling wave pattern, respectively.

ensemble of oscillators. As we have already pointed out, uniform random numbers between  $-1$  and  $1$  is chosen as initial conditions to obtain the discussed dynamical behaviors of Rössler oscillators. *PFC* states are not possible in the ensemble of Stuart-Landau oscillators for the initial conditions distributed between  $-1$  and  $1$ . On the other hand, if we prepare the initial conditions in the form of two cluster states (that is, half of the oscillators are provided  $+1$  as initial conditions and the other half as  $-1$  corresponding to the in-phase and out-of-phase states of *PFC*, the *PFC* states (two-cluster state) emerge even in the absence of nonlocal coupling, but only with the environmental coupling. However, the *PFC* shown in Figs. 15(a)-(b) is plotted for a finite value of nonlocal coupling  $\varepsilon = 0.005$  to break the permutation symmetry facilitated by the mean field global coupling, so that the state depicted in Figs. 15(a)-(b) cannot be simply regarded as a two cluster state. The values of the other parameters are the same as in Fig. 11. Upon increasing the strength of the nonlocal coupling  $\varepsilon$ , we have observed the chimera at the phase-flip transition (see Figs. 15(c)-(d)), solitary states (see Figs. 15(e)-(f)) and travelling wave pattern (see Figs. 15(g)-(h)). We have also depicted the variety of collective dynamical behaviors exhibited by the ensemble of identical Stuart-Landau oscillators in the two-parameter phase diagram (see Fig. 16) for the above choice of initial conditions in the form of two-cluster states.

#### 4. Conclusion

We have demonstrated the emergence of an interesting new type of chimera, where the two adjacent coherent domains exhibit out-of-phase synchronized oscillations similar to phase-flip transitions. The incoherent domain of the chimera is constituted by the asynchronous oscillators at the onset of the phase-flip transition among the coherent domains, where each domain exhibits phase synchronized oscillations. Such a set of coexisting out-of-phase synchronized adjacent coherent domains interspersed by asynchronous incoherent domains constitute a rich spatio-temporal behavior constituting a new type of chimera, namely chimera at the phase-flip transition. Such a dynamical behavior is observed only in the nonlocally coupled ensemble of identical oscillators with a common dynamic environmental coupling. The nonlocal coupling facilitates the emergence of the asynchronous incoherent domain at the onset of the phase-flip transition

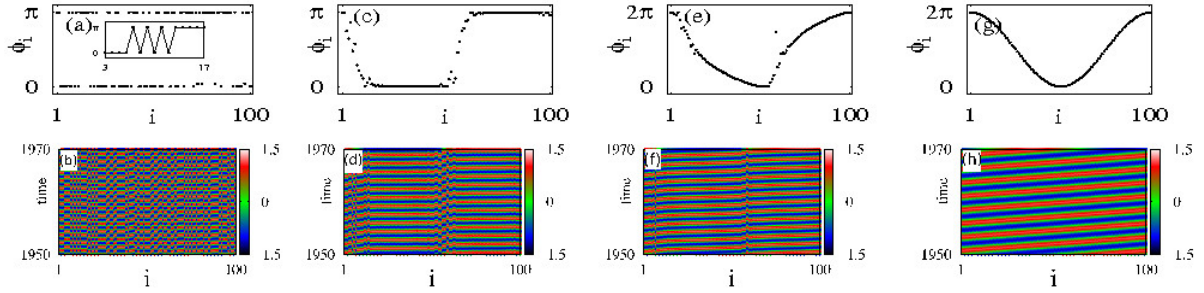


Figure 15: (Color online) Snapshots of the instantaneous phases  $\phi_i$  of the ensemble of Stuart-Landau oscillators for  $q = 0.8$  in the value nonlocal coupling (a)-(b)  $\epsilon = 0.005$ , (c)-(d)  $\epsilon = 0.05$ , (e)-(f)  $\epsilon = 0.13$  and (g)-(h)  $\epsilon = 0.22$  (initial condition in the form of cluster state). The values of the parameter are the same as in Fig. 11.

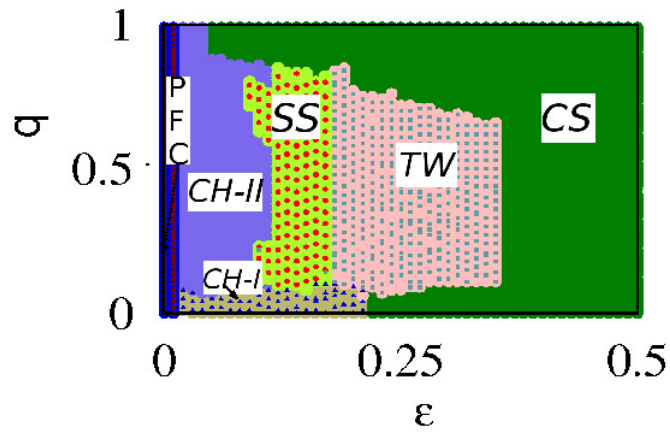


Figure 16: (Color online) Two parameter phase diagram as a function of the strength of the nonlocal coupling  $\epsilon \in (0, 0.5)$  and the strength of the mean field coupling  $q \in (0, 1)$  depicting different collective dynamical states of the ensemble of identical Stuart-Landau oscillators for specially prepared initial conditions in the form of two-cluster states. The parameter space marked as *PFC*, *CH-I*, *CH-II*, *SS*, *TW* and *CS* corresponds to the *PFC*, conventional chimera, chimera at phase-flip transition, solitary state, travelling wave pattern, and complete synchronized state, respectively.

among the ensemble of the identical oscillators. The dynamic environment coupling facilitates the onset of phase-flip transition in the ensemble of Rössler oscillators, while both the environmental and nonlocal couplings are required for the onset of phase-flip transition in the ensemble of Stuart-Landau oscillators. In the absence of the nonlocal coupling phase-flip transition will not be observed in the ensemble of identical Stuart-Landau oscillators. We have demonstrated the generic nature of our results using the paradigmatic Rössler and Stuart-Landau oscillators. In addition, a range of collective behaviors including clusters with phase-flip transition (*PFC*), conventional chimera, solitary states, coherent states, complete synchronization and travelling wave patterns are observed during the dynamical transitions as a function of the system parameters.

## Acknowledgments

The work of VKC forms part of a research project sponsored by INSA Young Scientist Project under Grant No. SP/YSP/96/2014. DVS is supported by the SERB-DST Fast Track scheme for young scientist under Grant No. ST/FTP/PS-119/2013 and CSIR Grant No. 03(1400)/17/EMR-II. ML is supported by a NASI Platinum Jubilee Senior Scientist Fellowship. He is also supported by a CSIR research project and a DST-SERB research project.

## Appendix A: Clusters with phase-flip transition (*PFC*) for other initial conditions

In order to confirm the robustness of clusters with phase-flip transition, they are shown using different sets of initial conditions. *PFC* emerging out of further two different sets of specific initial conditions  $x^2 + y^2 + z^2 = 1$  and  $\sin(\frac{\pi i}{N})$ , where  $i = 1, 2, 3, \dots, N$ , are depicted along with the transients in Figs .17(a) and (b), respectively. Further, we have also corroborated the robustness of the clusters with phase-flip transition by showing its existence for two more random initial conditions in Figs .17 (c) and (d). The initial conditions are uniform random numbers distributed between  $-p$  and  $q$ . Random numbers distributed symmetrically between  $p = q = 0.5$  are used to show *PFC* in Fig.17 (c) and whereas asymmetric distribution of random numbers between  $p = 0.5$ ,  $q = 1.5$  are used to depict the *PFC* in Fig.17 (d). These figures elucidate that such a cluster with phase-flip transition can always emerge in the presence of the dynamic environmental coupling and that they arise not due to the manifestation of a specific choice of initial conditions.

## Appendix B: Phase flip transition between two coupled Rössler oscillators

In order to examine the existence of phase-flip transition as reported in Ref [64], we also consider two coupled chaotic Rössler oscillators interacting through dynamic environment,

$$\begin{aligned}\dot{x}_i &= -y_i - z_i + \varepsilon(x_j - x_i), \\ \dot{y}_i &= x_i + ay_i, \\ \dot{z}_i &= b + z_i(x_i - c) + kw_i, \\ \dot{w}_i &= -\alpha w_i + 0.5z_i + \eta(q\bar{w} - w_i),\end{aligned}$$

where  $i, j = 1, 2$  and  $i \neq j$ . The parameters are  $\bar{w} = \sum_{i=1}^2 \frac{1}{2}w_i$ ,  $a = 0.165$ ,  $b = 0.4$  and  $c = 8.5$  are the system parameters and  $\eta = 2$ ,  $k = 24$ . We show that the results of in-phase and anti-phase synchronized states for the values of  $q$  and  $\alpha$  as shown in Figs .18(a)-(b) and .18(d)-(e) respectively. Therefore, the transition between the in-phase and out-of-phase synchronizations is studied numerically using the values of average phase-difference between the coupled oscillator systems. In this case, the instantaneous phase  $\phi_i$  of the  $i^{th}$  oscillator is defined as  $\phi_i = \arctan(y_i/x_i)$ , where  $x_i$  and  $y_i$  denote the state variables. The average

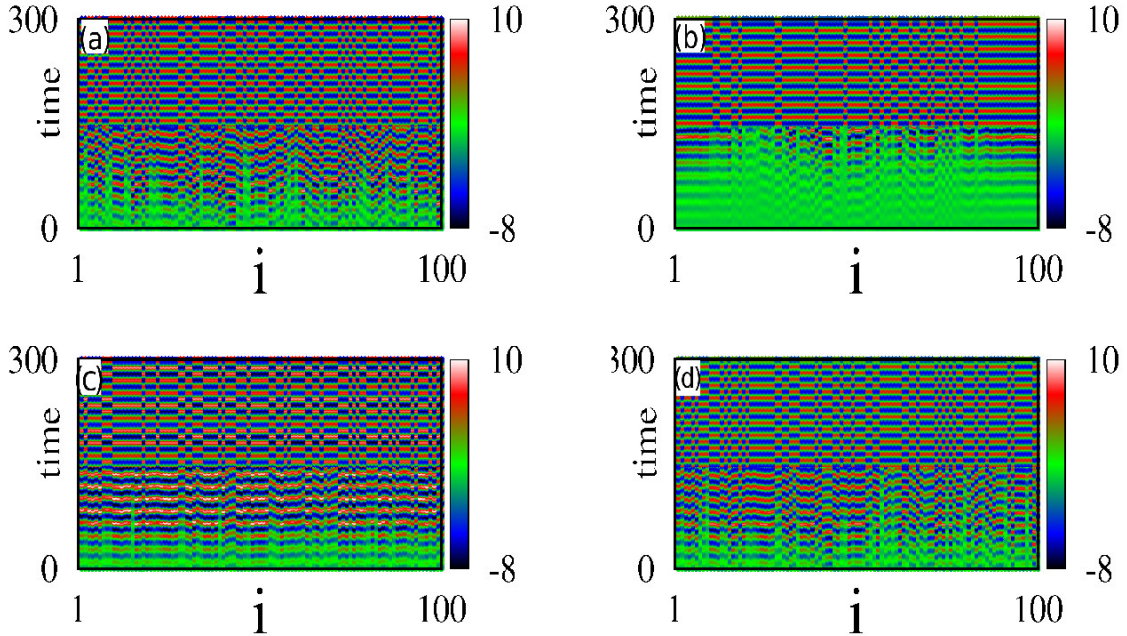


Figure .17: (Color online) Clusters with phase-flip transition (*PFC*) with transient behavior for further different sets of initial conditions (a)  $x^2 + y^2 + z^2 = 1$ , (b)  $\sin(\frac{\pi i}{N})$ , (c) symmetric distribution of uniform random numbers between  $p = q = 0.5$  and (d) asymmetric distribution of random numbers between  $p = 0.5$ ,  $q = 1.5$ . Other parameters are the same as in Fig 1(c)-(d).

phase difference between any two oscillators is  $\Delta\phi_{ij} = \langle |\phi_i - \phi_j| \rangle_t$ . The corresponding results of phase difference between the oscillators are also plotted as a function of  $q$  and  $\alpha$  as shown in Fig. .18(c) and (f), respectively.

### Appendix C: Bistability between two coupled Rössler oscillators

Now, we will demonstrate the emergence of bistability and the related bifurcations/transitions even between a system of two coupled Rössler oscillators among the in-phase and out-of-phase synchronized oscillations in order to substantiate our discussion on the observed multistability among  $N = 100$  oscillators. The bifurcation diagrams as functions of both the strength of the mean field interaction  $q$  and the strength of the nonlocal coupling  $\varepsilon$  are shown in Figs. .19(a) and (b), respectively. Figure .19(a) is depicted in the absence of any nonlocal coupling,  $\varepsilon = 0$ , while Fig. .19(b) is depicted for  $q = 0.2$ , where there is no bistability in the absence of nonlocal coupling as is evident from Fig. .19(a), in order to demonstrate that both the mean field and nonlocal couplings can induce bistability. Out-of-phase synchronized oscillations (represented by filled squares) are only stable in  $B_1$  and in-phase synchronized oscillations (represented by filled circles) are alone stable in  $B_3$  in both the figures, whereas in  $B_2$  both the out-of-phase synchronized and in-phase synchronized oscillations are stable thereby elucidating the emergence of bistability between two different states even in just two coupled oscillators. Therefore intuitively one will be able to realize that for  $N = 100$  coupled oscillators there exists a rich variety of multistability among the synchronized and desynchronized states thereby leading to the chimera states and solitary states discussed in Fig. 10. Transitions among the different states are better visualized for  $N = 100$  coupled oscillators as discussed in the main text.

### References

- [1] Kuramoto Y. *Chemical Oscillations, Waves, and Turbulence*. (Springer-Verlag., Berlin, 1984).

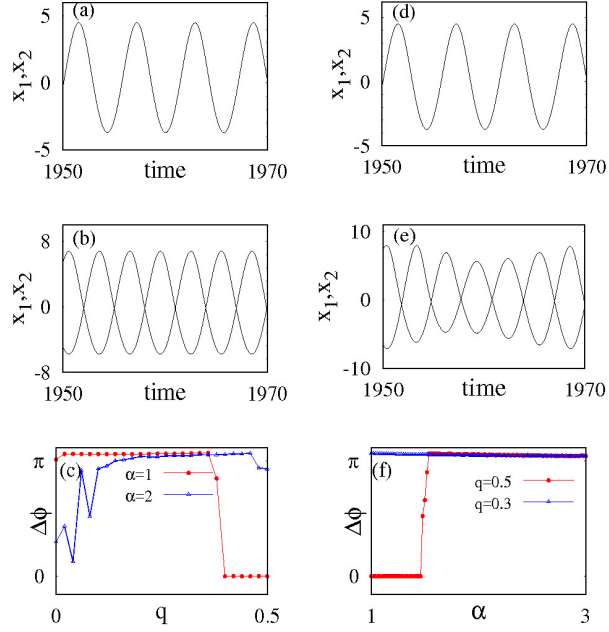


Figure .18: (Color online) In-phase (a)  $q = 0.5, \alpha = 1$ , (d)  $\alpha = 1, q = 0.4$  and out-of-phase transitions (b)  $q = 0.25, \alpha = 1$ , (e)  $\alpha = 2, q = 0.4$ . The phase difference between the two oscillators as a function of (c)  $q$  and (f)  $\alpha$  respectively.

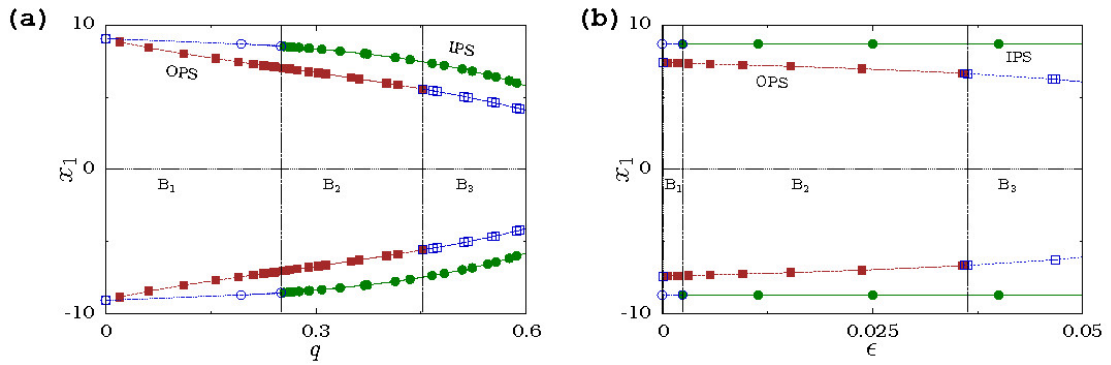


Figure .19: (Color online) Two coupled chaotic Rössler oscillators interacting through dynamic environment. Bifurcation diagram for varying the values of  $q$  (left) for fixed value of coupling strength  $\epsilon = 0$  and varying the values of  $\epsilon$  (right) for fixed value of  $q = 0.2$ . The unfilled symbols correspond to unstable states, while the filled symbols represent stable states. The filled circle and filled square represent the in-phase and out-of-phase synchronized states, respectively.

- [2] Pikovsky A, Rosenblum M, and Kurths J. *Synchronization: A Universal Concept in Nonlinear Sciences* (Cambridge University Press, Cambridge, England, 2001).
- [3] Boccaletti S, Kurths J, Osipov G, Valladares DL, Zhou CS, Physics Reports. 2002 ;366(1):1-102.
- [4] Winfree A T. *The Geometry of Biological Time* (Springer, New York, 2001).
- [5] Battogtokh D, and Kuramoto Y. Coexistence of coherence and incoherence in nonlocally coupled phase oscillators. *Nonlinear Phenom. Complex. Sys* 2002;5:80.
- [6] Abrams D M, and Strogatz S H. Chimera states for coupled oscillators. *Phys. Rev. Lett* 2004;93:174102.
- [7] Abrams D M, and Strogatz S H. Chimera states in a ring of nonlocally coupled oscillators. *Int. J. Bifur. Chaos* 2006;16:21.
- [8] Abrams D M, Mirollo R, Strogatz S H, and Wiley D A. Solvable model for chimera states of coupled oscillators. *Phys. Rev. Lett.* 2008;101:084103.
- [9] Sethia G C, Sen A, and Atay F.M. Clustered chimera states in delay-coupled oscillator systems. *Phys. Rev. Lett.* 2008;100:144102.
- [10] Laing C R. Chimeras in networks of planar oscillators. *Phys. Rev. E* 2010;81:066221.
- [11] Shima S I, and Kuramoto Y. Rotating spiral waves with phase-randomized core in nonlocally coupled oscillators. *Phys. Rev. E* 2004;69:036213.
- [12] Bordyugov G, Pikovsky A, and Rosenblum M. Self-emerging and turbulent chimeras in oscillator chains. *Phys. Rev. E* 2010;82:035205.
- [13] Martens E A, Laing C R, and Strogatz S H. Solvable model of spiral wave chimeras. *Phys. Rev. Lett.* 2010;104:044101.
- [14] Sheeba J H, Chandrasekar V K, and Lakshmanan M. Chimera and globally clustered chimera: impact of time delay. *Phys. Rev. E.* 79 2009;79:055203.
- [15] Shepelev I A, Zakharova A, Vadivasoa T E Chimera regimes in a ring of oscillators with local nonlinear interaction.. *Commun Nonlinear Sci Numer Simulat* 2017;44:277.
- [16] Omelchenko I, Maistrenko Y, Hövel P, and Schöll, E. Loss of coherence in dynamical networks: spatial chaos and chimera states. *Phys. Rev. Lett.* 2011;06:234102.
- [17] Omelchenko I, Riemenschneider B, Hövel P, Maistrenko Y, and Schöll E. Transition from spatial coherence to incoherence in coupled chaotic systems. *Phys. Rev. E* 2012;85:026212.
- [18] Panaggio M J, and Abrams D. M. Chimera states: coexistence of coherence and incoherence in networks of coupled oscillators. *Nonlinearity* 2015;R67:28.
- [19] Omelchenko I, Omelchenko O E, Hövel P, and Schöll E. When nonlocal coupling between oscillators becomes stronger: patched synchrony or multichimera states. *Phys. Rev. Lett.* 2013;110:224101.
- [20] Gopal R, Chandrasekar V K, Senthilkumar D V, Venkatesan A, and Lakshmanan M. Effect of asymmetry parameter on the dynamical states of nonlocally coupled nonlinear oscillators. *Phys. Rev. E* 2015;91:062916.
- [21] Dudkowski D, Maistrenko Y, and Kapitaniak T. Different types of chimera states: An interplay between spatial and dynamical chaos. *Phys. Rev. E.* 2014;90:032920 .
- [22] Zakharova A, Kapeller A, and Schöll E. Chimera Death: Symmetry Breaking in Dynamical Networks. *Phys. Rev. Lett* 2014;112:154101 .
- [23] Omelchenko I, Provata A, Hizanidis J, Schöll E. Robustness of chimera states for coupled FitzHugh-Nagumo oscillators. *Phys. Rev. E* 2015;91:022917.
- [24] Omelchenko I, Zakharova A, Hövel P, Sibert J, and Schöll E. Nonlinearity of local dynamics promotes multi-chimera states. *Chaos* 2015;25:083104.
- [25] Wai Lim Ku, Michelle G and Ott E. Dynamical transitions in large systems of mean field-coupled Landau-Stuart oscillators: Extensive chaos and cluster states. *Chaos* 2015;25:123122.
- [26] Schmidt L and Krischer K Clustering prerequisite for chimera states in globally coupled systems. *Phys. Rev. Lett* 2015;114:034101.
- [27] Semennova N, Zakharova A, Schöll E, and Anishchenko, V. Does hyperbolicity impede emergence of chimera states in networks of nonlocally coupled chaotic oscillators. *Europhys. Lett.* 2015;112:40002.
- [28] Bogomolov S A, Slepnev A V, Strelkova G I, E. Schöll and Anischenko V S. Mechanisms of appearance of amplitude and phase chimera states in ensembles of nonlocally coupled chaotic systems. *Commun Nonlinear Sci Numer Simulat* 2017;23:25-26.
- [29] Yeldesbay A, Pikovsky A, and Rosenblum M. Chimeralike States in an Ensemble of Globally Coupled Oscillators. *Phys. Rev. Lett.* 2014;112:144103.
- [30] Sethia G C, and Sen A. Chimera States: The Existence Criteria Revisited. *Phys. Rev. Lett.* 2014;112:144101.
- [31] Schmidt L, Schönleber K, Krischer K, and GarciáMorales V. Coexistence of synchrony and incoherence in oscillatory media under nonlinear global coupling. *Chaos* 2014;24:013102.
- [32] Premalatha K, Chandrasekar V K, Senthilvelan M, and Lakshmanan M. Impact of symmetry breaking in networks of globally coupled oscillators. *Phys. Rev. E* 2015;91:052915.
- [33] Loos S, Clawssen J, Schöll J C, and Zakharova A. Chimera patterns under the impact of noise. *Phys. Rev. E.* 2016;93:012209.
- [34] Larger L, Penkovsky B, and Maistrenko Y. Virtual Chimera States for Delayed-Feedback Systems. *Phys. Rev. Lett.* 2013;111:054103.
- [35] Semenov V, Zakharova A, Maistrenko Y, and Schöll E. Delayed-feedback chimera states: Forced multiclusters and stochastic resonance. *Euro. Phys. Lett.* 2016;115:1005.
- [36] Schöll E. Synchronization patterns and chimera states in complex networks: Interplay of topology and dynamics. *The European Physical Journal Special Topics* 2016;225:891-919.
- [37] Jaros P, Maistrenko Yu, and Kapitaniak T. Chimera states on the route from coherence to rotating waves. *Phys. Rev. E.*

- 2015;91:022907.
- [38] Kapitaniak T, Kuzma P, Wojewoda J, Czolczynski K and Maistrenko Y L. Imperfect chimera states for coupled pendula. *Sci. Rep.* 2014;4:6379.
- [39] Semenova N I, Rybalova E V, Strelkova G I and Anischenko V S. Coherence-incoherence transition in ensembles of nonlocally coupled oscillators with nonhyperbolic and hyperbolic attractors. *Regular and Chaotic Dynamics.* 2017;22:148-162.
- [40] Premalatha K, Chandrasekar V K, Senthilvelan M, and Lakshmanan M. Imperfectly synchronized states and chimera states in two interacting populations of nonlocally coupled Stuart-Landau oscillators. *Physical Review E* 2016;94:012311.
- [41] Jaros P, Brezetsky S, Levchenko R, Dudkowski D, Kapitaniak T, Maistrenko Y. Solitary states for coupled oscillators. *arXiv* 2017; preprint arXiv:1703.06950.
- [42] Maistrenko Yu, Penkovsky B, and Rosenblum M. Solitary state at the edge of synchrony in ensembles with attractive and repulsive interactions. *Phys. Rev. E* 2014;89:060901(R).
- [43] Gopal R, Chandrasekar V K, Venkatesan A, and Lakshmanan, M. Observation and characterization of chimera states in coupled dynamical systems with nonlocal coupling. *Phys. Rev. E.* 2014;89:052914.
- [44] Banerjee T, and Ghosh D. Transition from amplitude to oscillation death under mean-field diffusive coupling. *Phys. Rev. E* 2014; 89:052912.
- [45] Laing C R. Chimeras in networks with purely local coupling. *Phys. Rev. E* 2015;92:050904(R).
- [46] Bera B K, Ghosh D, and Lakshmanan M. Chimera states in bursting neurons. *Phys. Rev. E* 2016;93:012205.
- [47] Sethia G, Sen A, and Johnston G L. Amplitude-mediated chimera states. *Phys. Rev. E.* 2013;88:042917.
- [48] Chandrasekar V K, Gopal R, Venkatesan A, and Lakshmanan M. Mechanism for intensity-induced chimera states in globally coupled oscillators. *Phys. Rev. E.* 2014;90:062913.
- [49] Dutta P S and Banerjee T. Spatial coexistence of synchronized oscillation and death: A chimeralike state. *Phys. Rev. E* 2015;92:042919.
- [50] Schneider I, Kapeller M, Loos S, Zakharova A, Fiedler B, and Schöll E. Stable and transient multicluster oscillation death in nonlocally coupled networks. *Phys. Rev. E* 2015;92:052915.
- [51] Tinsley M R, Nkomo S, and Showalter S. Chimera and phase-cluster states in populations of coupled chemical oscillators. *Nat. Phys.* 2012;8:662.
- [52] Hagerstrom A M, Murphy T E, Roy R, Hövel P, Omelchenko I, and Schöll E. Experimental observation of chimeras in coupled-map lattices. *Nat. Phys.* 2012;8:658-661.
- [53] Nkoma S, Tinsley M R, and Showalter K. Chimera States in Populations of Nonlocally Coupled Chemical Oscillators. *Phys. Rev. Lett.* 2013;110:244102.
- [54] Martens E A, Thutupalli S, Fourrière A, and Hallatschek, O. Chimera states in mechanical oscillator networks. *Proc. Nat. Acad. Sci. USA,* 2013;110:10563.
- [55] Rottenberg N C, Amlaner C J, and Lima S L. Behavioral Neurophysiological and evolutionary perspectives on unihemispheric sleep. *Neurosci Biobehav Rev.* 2000;24:817.
- [56] Olbrich E, Claussen J C, and Achermann P. The sleeping brain as a complex system. *Phil. Trans. R. Soc. A* 2011;369:3884.
- [57] Olmi S, Martens E A, Thutupalli S and Torcini A. Intermittent chaotic chimeras for coupled rotators. *Phys. Rev. E* 2015;92:030901.
- [58] Olmi S. Chimera states in coupled Kuramoto oscillators with inertia. *Chaos* 2015;25:123125.
- [59] Filatrella G, Nielsen A H, and Pedersen N F. Analysis of a power grid using a Kuramoto-like model. *Eur. Phys. J. B* 61 2008;61(4):485.
- [60] Laing C R, and Chow C C. Stationary bumps in networks of spiking neurons. *Neural Computation* 2000;13:1473.
- [61] Nizhnik L P, Nizhnik I L, and Hasler M. Stable stationary solutions in reaction-diffusion systems consisting of a 1D array of bistable cells. *Int. J. Bif. Chaos.* 2002;12:261.
- [62] Harris-Warrick R M, et al., *Dynamics of Biological Networks.* (MIT Press, Cambridge, MA, 1992).
- [63] Resmi V, Ambika G, and Amritkar R E. Synchronized states in chaotic systems coupled indirectly through a dynamic environment. *Phys. Rev. E* 2010;81:046216.
- [64] Sharma A, Shrimali M D and Dana S K. Phase-flip transition in nonlinear oscillators coupled by dynamic environment. *Chaos* 2012;22:023147.
- [65] Sharma A, and Shrimali M D. Experimental realization of mixed-synchronization in counter-rotating coupled oscillators. *Nonlinear Dyn.* 2012;69:371.
- [66] Camilli A, and Bassler B L. Bacterial small-molecule signaling pathways. *Science* 328 2006;328:1113.
- [67] Li B M, Fu C, Zhang H, and Wang X. Synchronization and quorum sensing in an ensemble of indirectly coupled chaotic oscillators. *Phys. Rev. E* 2012;86:046207.
- [68] Cruz J M, Escalona J, Parmananda P, Karnatak R, Prasad A, and Ramaswamy R. Phase-flip transition in coupled electrochemical cells. *Phys. Rev. E* 2010;81:046213.
- [69] Prasad A, Kurths J, Dana S K, and Ramaswamy R. Phase-flip bifurcation induced by time delay. *Phys. Rev. E* 2006;74:035204;
- [70] Sharma A, Shrimali M D, Prasad A, Ramaswamy R, and Feudel U. Phase-flip transition in relay-coupled nonlinear oscillators. *Phys. Rev. E* 2011;84:016226.
- [71] McMillen D, Kopell N, Hasty J, and Collins J J. Synchronizing genetic relaxation oscillators by intercell signaling. *Proc. Natl. Acad. Sci. USA* 2002;99:679.
- [72] Chandrasekar V K, Gopal R, Senthilkumar D V, and Lakshmanan M. Phase-flip chimera induced by environmental nonlocal coupling. *Phys. Rev. E* 2016;94:012208.
- [73] Taylor A F, Tinsley M R, Wang F, Huang Z, and Showalter K. Dynamical Quorum Sensing and Synchronization in

- Large Populations of Chemical Oscillators. *Science* 2009;323:164.
- [74] Strogatz S H From Kuramoto to Crawford: exploring the onset of synchronization in populations of coupled oscillators. *Physica D* 2000;143:1.
  - [75] Restrepo J G, Ott E, and Hunt B R Synchronization in large directed networks of coupled phase oscillators. *Chaos* 2006;015017:16.
  - [76] Chen A. Modeling a synthetic biological chaotic system relaxation oscillators coupled by quorum sensing. *Nonlinear Dyn* 2011;63:711.
  - [77] Gao L, Hu M, Xu Z, Hu A. Synchronization and chaos control by quorum sensing mechanism. *Nonlinear Dyn* 2013;73:1253.
  - [78] Ullner E, Zaikin A, Volkov E, and Ojalvo J G. Multistability and clustering in a population of synthetic genetic oscillators via phase-repulsive cell-to-cell communication. *Phys. Rev. Lett.* 2007;99:148103.